JOURNAL OF Materials CHEMISTRY

Synthesis and characterisation of a layered organically-templated manganese phosphate, $[Mn_2(HPO_4)_3]\cdot(NH_3(CH_2)_2NH_3)_{3/2}\cdot H_2PO_4$, and its reaction with water†

Ann M. Chippindale,*[a] Fabrice O. M. Gaslain,[a] Andrew R. Cowley[b] and Anthony V. Powell[c]

[a]*Department of Chemistry, The University of Reading, Whiteknights, Reading, Berks, UK RG6 6AD. E-mail: a.m.chippindale@rdg.ac.uk*
[b]*Chemical Crystallography Laboratory, 9 Parks Road, Oxford, UK OX1 3PD*
[c]*Department of Chemistry, Heriot-Watt University, Riccarton, Edinburgh, UK E14 4AS*

Received 22nd May 2001, Accepted 26th September 2001
First published as an Advance Article on the web 29th October 2001

A new layered manganese(II) phosphate, $[Mn_2(HPO_4)_3]\cdot(NH_3(CH_2)_2NH_3)_{3/2}\cdot H_2PO_4$, has been synthesised under solvothermal conditions at 433 K in the presence of ethylenediamine and the structure determined at 150 K using single-crystal X-ray diffraction data ($M_r = 587.95$, triclinic, space group, $P\bar{1}$, $a = 6.651(1)$, $b = 9.343(1)$, $c = 14.512(2)$ Å, $\alpha = 87.687(3)$, $\beta = 84.096(4)$, $\gamma = 89.066(4)^\circ$, $V = 896.20$ Å^3, $Z = 2$, $R = 0.0409$ and $R_w = 0.0462$ for 2939 observed data ($I > 3(\sigma(I))$). The structure consists of anionic manganese-phosphate layers of formula $[Mn_2(HPO_4)_3]^{2-}$ containing *trans* edge sharing chains of MnO_6 octahedra linked *via* MnO_5 and HPO_4 polyhedra. $H_2PO_4^-$ and $(NH_3(CH_2)_2NH_3)^{2+}$ ions lie between the manganese-phosphate layers. Magnetic measurements indicate Curie–Weiss paramagnetism above 25 K with $\mu_{eff} = 5.77(1)\ \mu_B$ and $\theta = -30(1)$ K, consistent with the presence of high-spin Mn^{2+} ions and antiferromagnetic interactions. The latter result in magnetic ordering at $T_N = 2.5(1)$ K. The temperature dependence of the susceptibility can be successfully fitted assuming a triangular antiferromagnetic lattice of $S = 5/2$ spins, yielding an exchange parameter J/k of $-0.72(1)$ K and a g-value of 1.930(3). On treatment with water, a phase of composition $[Mn_2(HPO_4)_3]\cdot(NH_3(CH_2)_2NH_3)\cdot(H_2O)_x$ ($x \sim 0.2$) is formed with retention of the MnPO layers but removal of the interlayer $H_2PO_4^-$ groups.

Introduction

There has recently been much interest in the synthesis of microporous metal phosphates because of their potential uses in catalysis and ion exchange. Although attention focused initially on the phosphates of aluminium (AlPOs) and gallium (GaPOs) because of their structural similarities to zeolites (aluminosilicates) and clays, numerous open-framework transition-metal phosphates are now also known.[1] In particular, many 3-dimensional and layered examples containing V, Fe, Co and Zn in a range of coordination geometries have been synthesised in the presence of organic 'templates' such as amines or diamines. Less work has been done to date however on analogous phosphates incorporating manganese. Although a few 3-D open-framework MnAPOs[2] and MnGaPOs[3–8] have been characterised recently, there are only two structural reports in the literature of templated MnPOs, namely $[Mn_2(PO_4)_3](NH_3(CH_2)_2NH_3)(H_2O)$[9] and $[Mn_6(HPO_4)_4(PO_4)_2]\cdot(C_4N_2H_{12})(H_2O)$,[10] which have 2-D structures in which manganese-phosphate layers are separated by ethylenediammonium and piperazinium cations respectively.

Here we describe the synthesis and characterisation of $[Mn_2(HPO_4)_3]\cdot(NH_3(CH_2)_2NH_3)_{3/2}\cdot H_2PO_4$, a new ethylenediamine templated MnPO. The manganese-phosphate layers are similar to those found previously by Escobal *et al.* in $[Mn_2(PO_4)_3](NH_3(CH_2)_2NH_3)(H_2O)$,[9] but the interlayer void contains $H_2PO_4^-$ units as well as ethylenediammonium cations. Treatment of $[Mn_2(HPO_4)_3]\cdot(NH_3(CH_2)_2NH_3)_{3/2}\cdot H_2PO_4$ with water produces a second layered material, $[Mn_2(HPO_4)_3]\cdot(NH_3(CH_2)_2NH_3)\cdot(H_2O)_x$ ($x \sim 0.2$), with retention of the original manganese-phosphate layers but removal of the interlayer $H_2PO_4^-$ polyhedra and some of the ethylenediamine cations.

Experimental

Characterisation methods

Powder X-ray diffraction patterns for all products were recorded on a Siemens D5000 diffractometer (graphite-monochromated Cu-Kα radiation ($\lambda = 1.5418$ Å)). Energy-dispersive X-ray emission analyses (Mn : P ratios) were determined using a Philips CM20 transmission electron microscope with $Mn_2P_2O_7$[11] as calibration standard. Infrared spectra of samples diluted in KBr discs were recorded on a Perkin Elmer FTIR 1720-X spectrometer. Thermal analyses were performed either in air or dry N_2 using a Stanton Redcroft STA1000 thermal analyser with a heating rate of 4 K min^{-1} over the temperature range 300–1100 K. Magnetic susceptibility measurements for samples contained in gelatin capsules were made using a Quantum Design MPMS2 SQUID magnetometer. Data were collected over the temperature range $1.7 \leqslant T/K \leqslant 300$, both after cooling in zero applied field (zfc) and in the measuring field of 1000 G (fc). Data were corrected for the diamagnetism of the sample capsule and for intrinsic core diamagnetism.

†Electronic supplementary information (ESI) available: thermal ellipsoid plots of the manganese complex cation, phosphate anion and ethylenediammonium cation; IR spectra of $[Mn_2(HPO_4)_3]\cdot(NH_3(CH_2)_2NH_3)_{3/2}\cdot H_2PO_4$ and $[Mn_2(HPO_4)_3]\cdot(NH_3(CH_2)_2NH_3)\cdot(H_2O)_x$. See http://www.rsc.org/suppdata/jm/b1/b104491p/

 DOI: 10.1039/b104491p

Synthesis and preliminary characterisation of $[Mn_2(HPO_4)_3]\cdot(NH_3(CH_2)_2NH_3)_{3/2}\cdot H_2PO_4$

$[Mn_2(HPO_4)_3]\cdot(NH_3(CH_2)_2NH_3)_{3/2}\cdot H_2PO_4$ was prepared both as single crystals and pure, polycrystalline powder using solvothermal reactions. Single crystals were produced in reaction (i) from a gel of composition $MnCl_2\cdot 4H_2O : 49\ HO(CH_2)_2OH : 4.9\ NH_2(CH_2)_2NH_2 : 0.29\ Si(OEt)_4 : 10\ H_3PO_4$(aq). 0.43 g $MnCl_2\cdot 4H_2O$ were dispersed in 6 cm^3 ethylene glycol by vigorous stirring and 0.7 cm^3 ethylenediamine added together with 0.15 cm^3 $Si(OEt)_4$ as crystallising agent. After further stirring, 1.5 cm^3 aqueous H_3PO_4 (85% by weight) was added and the mixture sealed in a Teflon-lined autoclave and heated for 7 days at 433 K. The solid product consisted of colourless plate-like crystals of the title compound, block-like crystals of ethylenediamine hydrogenphosphate[12] and a small amount of white polycrystalline material. A plate was studied by single-crystal X-ray diffraction as described below and found to have the composition $[Mn_2(HPO_4)_3]\cdot(NH_3(CH_2)_2NH_3)_{3/2}\cdot H_2PO_4$. Washing a portion of the product in distilled water led to disintegration of the crystals (*vide infra*). The remaining product was washed first in concentrated acetic acid and then methanol, a procedure which removed the ethylenediamine hydrogenphosphate but left the crystals of the title compound intact. The powder X-ray diffraction pattern of the resulting product could be indexed on the basis of the triclinic unit cell obtained from the single-crystal study with the exception of four weak peaks (*d* values: 9.823, 6.549, 4.361, 2.957 Å). Combustion analysis (measured, C: 5.77, H: 3.36, N: 6.27%; calculated for $[Mn_2(HPO_4)_3]\cdot(NH_3(CH_2)_2NH_3)_{3/2}\cdot H_2PO_4$, C: 6.13, H: 3.43, N: 7.15%) gave a C : N ratio of *ca.* 1 suggesting that ethylenediamine remains intact in all phases present.

A pure polycrystalline sample of $[Mn_2(HPO_4)_3]\cdot(NH_3(CH_2)_2NH_3)_{3/2}\cdot H_2PO_4$ was prepared from reaction (ii) by applying the same synthetic and 'work-up' procedures as above to a starting gel of composition $MnCl_2\cdot 4H_2O : 66.5\ HO(CH_2)_2OH : 5.2\ NH_2(CH_2)_2NH_2 : 0.3\ Si(OEt)_4 : 10.2\ H_3PO_4$(aq) (requiring 0.32 g, 6 cm^3, 0.56 cm^3, 0.1 cm^3 and 1.13 cm^3 of the reagents respectively). All peaks in the powder X-ray diffraction pattern of the resulting pale-pink product (Table 1) could be indexed on a triclinic unit cell with lattice parameters: $a = 6.655(2)$, $b = 9.341(3)$ and $c = 14.510(2)$ Å; $\alpha = 87.680(1)$, $\beta = 84.10(2)$ and $\gamma = 89.066(1)^\circ$. Analytical electron microscopy showed that each crystallite examined contained Mn and P, but no Si. The Mn : P ratio of 0.47(3) is in good agreement with the value of 0.5 obtained from the single-crystal study. Combustion analysis values of C: 6.15, H: 3.50, N: 6.98% agree well with the calculated values above, further confirming that the sample is monophasic. An IR spectrum of the compound showed features consistent with the presence of ethylenediammonium cations[13] with broad bands occurring in the region 3200–2800 cm^{-1} corresponding to N–H stretching modes and the two sharp bands at 1640 and 1534 cm^{-1} assignable as antisymmetric and symmetric $-NH_3^+$ deformation modes respectively. Over the range 1400–900 cm^{-1} there are a number of sharp bands arising from –O–H and $-CH_2-$ bending and P–O stretching modes, but unambiguous individual assignments are not possible. Thermal analysis in air revealed a sharp weight loss (*ca.* 6%) at 523 K and a gradual weight loss (*ca.* 11%) over the range 523–700 K which may correspond to losses of 0.5 and 1 mole of ethylenediamine respectively (calculated values of 5.1 and 10.2%). Collapse of the framework occurred above ~725 K to give an amorphous residue.

Magnetic susceptibility measurements were made using ~40 mg of powdered $[Mn_2(HPO_4)_3]\cdot(NH_3(CH_2)_2NH_3)_{3/2}\cdot H_2PO_4$.

Table 1 Powder X-ray diffraction data for $[Mn_2(HPO_4)_3]\cdot(NH_3(CH_2)_2NH_3)_{3/2}\cdot H_2PO_4$

Relative intensity	$2\theta_{obs}$/°	d_{obs}/Å	d_{calc}/Å	h	k	l
100	6.105	14.465	14.422	0	0	1
3	9.462	9.339	9.333	0	1	0
1	11.108	7.959	7.979	0	1	1
3	11.505	7.685	7.699	0	−1	1
11	12.252	7.218	7.211	0	0	2
1	13.300	6.652	6.619	1	0	0
1	14.147	6.255	6.263	1	0	1
1	15.209	5.821	5.817	0	1	2
2	16.504	5.367	5.368	1	−1	0
1	16.831	5.263	5.271	1	1	1
1	17.238	5.140	5.145	1	0	2
1	18.493	4.794	4.807	0	0	3
1	19.035	4.659	4.666	0	2	0
3	20.436	4.342	4.343	0	1	3
2	21.492	4.131	4.132	−1	−1	2
2	21.750	4.083	4.094	1	0	3
1	22.308	3.982	3.989	0	2	2
4	23.403	3.798	3.794	1	2	1
2	24.134	3.685	3.692	1	−2	1
6	24.693	3.602	3.605	0	0	4
1	25.266	3.522	3.522	1	2	2
1	25.556	3.483	3.478	−1	1	3
1	26.089	3.413	3.415	0	2	3
1	26.946	3.306	3.309	2	0	0
1	27.299	3.264	3.265	−1	−2	2
1	28.213	3.160	3.163	1	1	4
1	28.767	3.101	3.107	2	−1	0
1	29.074	3.069	3.066	0	3	1
1	29.779	2.998	2.995	2	1	2
6	30.988	2.883	2.884	0	0	5
2	31.769	2.814	2.817	0	−3	2
1	32.228	2.775	2.771	−2	1	2
1	32.899	2.720	2.722	2	2	1
1	33.691	2.658	2.660	0	3	3
1	34.301	2.612	2.611	−2	2	1
1	35.075	2.556	2.550	−1	0	5
1	35.500	2.527	2.527	1	3	3
1	35.837	2.504	2.504	2	1	4
1	36.529	2.458	2.457	2	−1	4
1	37.384	2.404	2.404	0	0	6
1	38.654	2.327	2.326	1	−2	5
1	39.393	2.285	2.285	−2	2	3
1	39.769	2.265	2.267	−1	2	5
1	40.083	2.248	2.248	2	1	5
1	40.781	2.211	2.210	−1	−2	5
1	41.123	2.193	2.192	1	4	0
1	41.546	2.172	2.172	0	2	6
1	43.121	2.096	2.096	−3	−1	1
1	43.923	2.060	2.060	0	0	7

[a]Refined triclinic lattice parameters at 293 K ($0 \leqslant 2\theta \leqslant 45^\circ$): $a = 6.655(2)$, $b = 9.341(3)$ and $c = 14.510(2)$ Å; $\alpha = 87.680(1)$, $\beta = 84.10(2)$ and $\gamma = 89.066(1)^\circ$. (Cu Kα_1 radiation, $\lambda = 1.54056$ Å).

Treatment of $[Mn_2(HPO_4)_3]\cdot(NH_3(CH_2)_2NH_3)_{3/2}\cdot H_2PO_4$ with water

A sample of the polycrystalline sample from reaction (ii) was washed in distilled water, filtered and dried at room temperature. The powder X-ray diffraction pattern of the resulting pale-pink product showed that none of the original material remained (complete disappearance of the most intense line at *d* spacing 14.47 Å) but that a new crystalline phase with most intense line at $d = 11.02$ Å had been formed. The X-ray pattern could be indexed on the basis of an *A*-centred monoclinic cell ($a = 6.631(7)$, $b = 9.350(3)$, $c = 22.033(10)$ Å, $\beta = 90.54(8)^\circ$) (Table 2) with similar *a* and *b* lattice parameters to those of $[Mn_2(HPO_4)_3]\cdot(NH_3(CH_2)_2NH_3)_{3/2}\cdot H_2PO_4$ suggesting that the materials are structurally related and that the manganese-phosphate layers have been preserved on washing.

Analytical electron microscopy gave a Mn : P ratio of 0.64(6), in good agreement with the value of 0.67 predicted

Table 2 Powder X-ray diffraction data for $[Mn_2(HPO_4)_3]\cdot(NH_3(CH_2)_2NH_3)\cdot(H_2O)_x$

Relative intensity	$2\theta_{obs}$/°	d_{obs}/Å	d_{calc}/Å	h	k	l
100	8.019	11.016	11.016	0	0	2
7	10.306	8.576	8.607	0	1	1
1	15.218	5.817	5.778	0	1	3
1	16.123	5.493	5.508	0	0	4
5	16.873	5.250	5.243	1	1	1
2	20.543	4.319	4.304	0	2	2
4	23.299	3.815	3.820	1	2	0
6	24.231	3.670	3.672	0	0	6
1	26.141	3.406	3.403	1	1	5
2	26.910	3.310	3.315	2	0	0
1	28.341	3.146	3.147	−1	2	4
2	28.898	3.087	3.086	0	3	1
3	31.117	2.872	2.869	0	3	3
3	32.489	2.754	2.754	0	0	8
1	35.340	2.538	2.538	2	1	5
1	40.914	2.204	2.203	0	0	10
1	41.998	2.150	2.151	0	4	4
1	49.650	1.835	1.836	2	3	7
1	56.624	1.624	1.624	2	5	1

[a]Refined monoclinic lattice parameters at 293 K ($0 \leqslant 2\theta \leqslant 60$)°: $a = 6.631(7)$, $b = 9.350(3)$ and $c = 22.033(10)$ Å; $\beta = 90.54(8)$° (Cu Kα_1 radiation, $\lambda = 1.54056$ Å).

Table 3 Crystallographic data for $[Mn_2(HPO_4)_3]\cdot(NH_3(CH_2)_2NH_3)_{3/2}\cdot H_2PO_4$

Formula	$C_3H_{20}Mn_2N_3O_{16}P_4$
M_r	587.97
Crystal size (mm)	$0.1 \times 0.4 \times 0.4$
Crystal habit	colourless plate
Crystal system	Triclinic
Space group	$P\bar{1}$
a/Å	6.651(1)
b/Å	9.343(1)
c/Å	14.512(1)
α/°	87.687(3)
β/°	84.096(4)
γ/°	89.066(4)
Cell volume/Å^3	896.20
Z	2
Temperature/K	150
ρ_{calc}/g cm^{-3}	2.18
$\mu_{Mo\text{-}K\alpha}$/cm^{-1}	17.9
Unique data	3488
Observed data ($I > 3\sigma(I)$)	2939
R_{merge}	0.032
Residual electron density (min, max)/e Å^{-3}	−0.82, 0.80
Number of parameters refined	329
R	0.0409
R_w	0.0462

for retention of the $[Mn_2(HPO_4)_3]^{2-}$ layers. The IR spectrum confirmed that ethylenediammonium cations were present and the presence of a small amount of water could not be ruled out. Combustion analysis values of C: 5.57, H: 3.66, N: 6.04% with a C : N ratio of *ca.* 1 indicate that one mole of ethylenediamine is present per manganese-phosphate layer. The proposed formula is therefore $[Mn_2(HPO_4)_3]\cdot(NH_3(CH_2)_2NH_3)\cdot(H_2O)_x$ (x estimated from TGA to be *ca.* 0.2).

Single-crystal X-ray analysis of $[Mn_2(HPO_4)_3]\cdot(NH_3(CH_2)_2NH_3)_{3/2}\cdot H_2PO_4$

A colourless plate was selected from the unwashed product of reaction (i) and mounted on a nylon fibre using a drop of perfluoropolyether oil. It was then rapidly cooled to 150 K in a flow of cold nitrogen using an Oxford Cryosystems CRYOSTREAM cooling system. Data were collected on an Enraf-Nonius DIP2020 diffractometer using graphite-monochromated Mo-Kα radiation ($\lambda = 0.71069$ Å). Images were processed using the DENZO and SCALEPACK suite of programs.[14] Data were corrected for Lorentz and polarisation effects and a partial absorption correction applied by multiframe scaling of the image-plate data using equivalent reflections. Full experimental information is given in Table 3.

The structure was solved in the space group $P\bar{1}$ (No. 2)[15] by direct methods (SIR-92)[16] and all non-hydrogen atoms of the manganese-phosphate layer located. In addition, an approximately tetrahedral group of atoms was located in the interlayer space and assigned as an extra-framework PO_4 group. All Fourier calculations and subsequent least-squares refinement were performed using the CRYSTALS program suite.[17] The carbon and nitrogen atoms of two crystallographically distinct amine cations were located in difference Fourier maps. Full-matrix least-squares refinement of the coordinates and anisotropic thermal parameters of all non-hydrogen atoms converged satisfactorily, but the thermal parameters of the O atoms of the extra-framework PO_4 group and a nearby $-CH_2NH_3$ group of one of the organic cations were observed to be unusually large. Both these PO_4 and $-CH_2NH_3$ groups were subsequently modelled as disordered over 2 crystallographically-inequivalent positions. After refinement of the coordinates of the disordered atoms, it became apparent that for each position of the $-CH_2NH_3$ group there was an N···O distance to an O atom of one of the two PO_4 sites sufficiently short as to indicate the presence of hydrogen bonding. The site occupancies of the two positions of both groups were then refined, subject to the constraints that the occupancies of $-CH_2NH_3$ and PO_4 groups related by hydrogen bonding were identical and that the sum of the site occupancies of each group was unity. Subsequent refinement of the anisotropic thermal parameters of the disordered groups showed that the phosphate P atom was also disordered and this was included in the model.

Full-matrix least-squares refinement on F of atomic coordinates and anisotropic thermal parameters of non-hydrogen atoms converged satisfactorily. No geometric restraints were necessary. Each of the 3 crystallographically-distinct framework PO_4 groups was observed to have a long terminal P–O bond typical of a hydroxyl group. This assignment was confirmed by location of the H atoms in difference Fourier maps and subsequent refinement of their atomic coordinates (subject to restraint of the O–H bond lengths to 1.00(5) Å). The interlayer phosphate must be present as $H_2PO_4^-$ in order to achieve charge balance, although the hydrogen atoms could not be located. The hydrogen atoms of the ethylenediammonium cations were positioned geometrically between each cycle. A Chebyshev 3-term polynomial weighting scheme was applied giving final residuals of $R = 0.0409$ and $R_w = 0.0462$. Atomic coordinates and isotropic thermal parameters are given in Table 4 while selected interatomic distances and bond angles are given in Table 5 and the local coordination of the framework atoms is shown in Fig. 1.

CCDC reference number 171710. See http://www.rsc.org/suppdata/jm/b1/b104491p/ for crystallographic data in CIF or other electronic format.

Results and discussion

Crystal structure of $[Mn_2(HPO_4)_3]\cdot(NH_3(CH_2)_2NH_3)_{3/2}\cdot H_2PO_4$

The structure of $[Mn_2(HPO_4)_3]\cdot(NH_3(CH_2)_2NH_3)_{3/2}\cdot H_2PO_4$ consists of anionic layers of composition $[Mn_2(HPO_4)_3]^{2-}$ constructed from MnO_6, MnO_5 and HPO_4 polyhedra with ethylenediammonium cations and hydrogenphosphate anions residing within the interlayer spaces. The manganese-phosphate layers are very similar to those observed previously in

Table 4 Fractional atomic coordinates, isotropic thermal parameters ($Å^2$) and site occupancies for $[Mn_2(HPO_4)_3]\cdot(NH_3(CH_2)_2NH_3)_{3/2}\cdot H_2PO_4$

Atom	*x*	*y*	*z*	*U*(iso)	Occ.[a]
Mn(1)	0	0	0	0.0085	
Mn(2)	0.5	0	0	0.0080	
Mn(3)	0.23579(7)	0.32632(4)	−0.00413(3)	0.0094	
P(1)	0.2263(1)	0.14676(7)	0.17667(5)	0.0106	
P(2)	0.2749(1)	0.15940(7)	−0.18092(5)	0.0110	
P(3)	0.2667(1)	−0.30714(7)	−0.02706(5)	0.0084	
P(4)	0.536(2)	0.290(1)	0.4505(7)	0.0500	0.330(4)
P(5)	0.5233(9)	0.3141(6)	0.4270(3)	0.0172	0.670(4)
O(1)	0.2343(3)	0.0443(2)	0.0962(1)	0.0111	
O(2)	0.2021(3)	0.3019(2)	0.1428(1)	0.0111	
O(3)	0.4171(4)	0.1300(2)	0.2276(1)	0.0155	
O(4)	0.0382(4)	0.1106(2)	0.2467(2)	0.0176	
O(5)	0.2647(3)	0.0543(2)	−0.0958(1)	0.0127	
O(6)	0.2732(4)	0.3145(2)	−0.1505(1)	0.0130	
O(7)	0.1074(4)	0.1341(2)	−0.2416(2)	0.0177	
O(8)	0.4846(4)	0.1369(2)	−0.2397(2)	0.0167	
O(9)	0.4476(3)	−0.2299(2)	0.0043(1)	0.0101	
O(10)	0.0687(3)	−0.2252(2)	−0.0011(2)	0.0106	
O(11)	0.2494(3)	−0.4588(2)	0.0112(2)	0.0133	
O(12)	0.3024(4)	−0.3150(2)	−0.1366(2)	0.0162	
O(13)	0.705(1)	0.3806(8)	0.4795(6)	0.0500	0.330(4)
O(14)	0.546(1)	0.1340(8)	0.4735(5)	0.0500	0.330(4)
O(15)	0.327(1)	0.3512(8)	0.4926(5)	0.0186	0.330(4)
O(16)	0.546(1)	0.3170(7)	0.3410(5)	0.0225	0.330(4)
O(17)	0.4830(7)	0.4629(5)	0.3863(3)	0.0253	0.670(4)
O(18)	0.3599(8)	0.2043(7)	0.3986(3)	0.0262	0.670(4)
O(19)	0.4734(8)	0.3042(6)	0.5339(3)	0.0241	0.670(4)
O(20)	0.7304(7)	0.2586(4)	0.3950(3)	0.0317	0.670(4)
N(1)	0.1930(7)	0.0453(5)	0.5777(2)	0.0381	
N(2)	−0.0854(5)	0.4547(3)	0.2582(2)	0.0238	
N(3)	0.224(2)	0.655(1)	0.1952(9)	0.0192	0.330(4)
N(4)	0.3654(7)	0.5430(4)	0.2174(3)	0.0313	0.670(4)
C(1)	−0.0037(7)	0.0439(4)	0.5433(3)	0.0311	
C(2)	0.0350(6)	0.5398(4)	0.3164(3)	0.0260	
C(3)	0.245(2)	0.577(2)	0.2846(9)	0.0239	0.330(4)
C(4)	0.1896(9)	0.6336(7)	0.2528(6)	0.0340	0.670(4)
H(1)[b]	−0.019(9)	0.018(5)	0.243(4)	0.0500	
H(2)[b]	0.520(9)	0.038(4)	−0.241(4)	0.0500	
H(3)[b]	0.379(8)	−0.236(5)	−0.159(4)	0.0500	

[a]Occupancy is 1.00 unless otherwise stated. [b]Involved in chemical restraint.

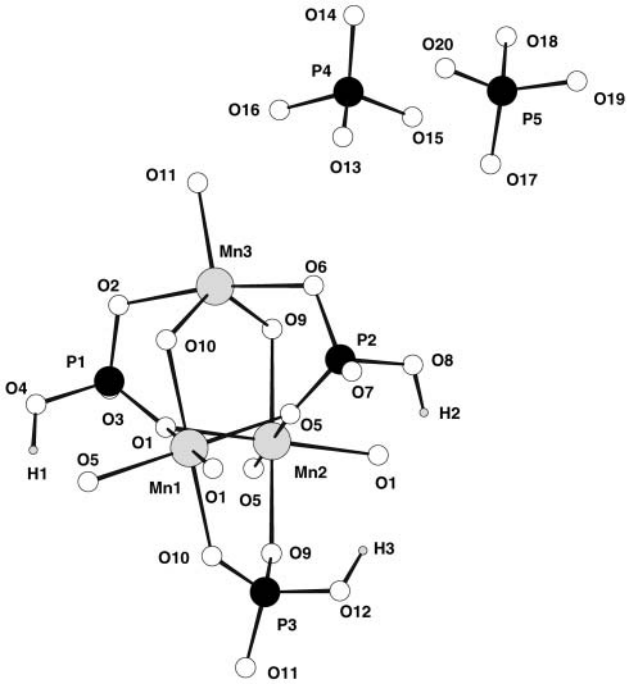

Fig. 1 Local coordination of the framework atoms and interlayer $H_2PO_4^-$ groups of $[Mn_2(HPO_4)_3]\cdot(NH_3(CH_2)_2NH_3)_{3/2}\cdot H_2PO_4$ showing the atom numbering scheme (drawing package: CAMERON[18]).

$[Mn_2(HPO_4)_3](NH_3(CH_2)_2NH_3)(H_2O)$.[9] Two of the three crystallographically-distinct Mn sites (Mn(1) and Mn(2)) occupy inversion centres and are octahedrally-coordinated to six oxygen atoms (Mn(1)–O_{av} = 2.192 Å, Mn(2)–O_{av} = 2.199 Å). The third Mn site (Mn(3)) has no crystallographic symmetry and is 5-coordinate with a geometry intermediate between square pyramidal and trigonal bipyramidal (Mn(3)–O_{av} = 2.159 Å) and similar to that observed previously in MnGaPO-2.[5] Bond-valence calculations[19] suggest that the manganese is present on all three sites as Mn^{2+} and this is further confirmed by the magnetic measurements below.

The $Mn(1)O_6$ and $Mn(2)O_6$ octahedra are linked *via trans* edges (Fig. 2). $Mn(3)O_5$ units bridge adjacent octahedra to form zigzag continuous chains running parallel to the crystallographic *a* axis. Two of the three crystallographically-distinct HPO_4 groups lie above and below the manganese-oxide chains and each connects an MnO_5 unit to one of the oxygens involved in the edge sharing of the MnO_6 octahedra. In addition to the bridging oxygens, both phosphorus atoms carry two terminal oxygen atoms, one of which is protonated (P(1)–O(4)H, 1.561(2) Å and P(2)–O(8)H, 1.574(2) Å) and one of which has a rather shorter phosphorus–oxygen distance implying some degree of multiple bonding (P(1)–O(3), 1.535(2) Å and P(2)–O(7), 1.516(2) Å). The third HPO_4 group forms cross-linkages between neighbouring chains by being linked to one chain through a single oxygen atom and to the other through two oxygens. The remaining terminal oxygen atom is present as a hydroxyl group (P(3)–O(12), 1.588(2) Å). The three P–OH groups are involved in strong intralayer hydrogen bonding interactions to neighbouring phosphoryl groups (O(4)H···O(7), 2.505(3); O(8)H···O(3), 2.571(3); O(12)H···O(3), 2.762(3) Å). With the exception of the oxygens in the five terminal P–O groups and that of the Mn(3)–O(11)–P(3) bridge, all the remaining oxygens

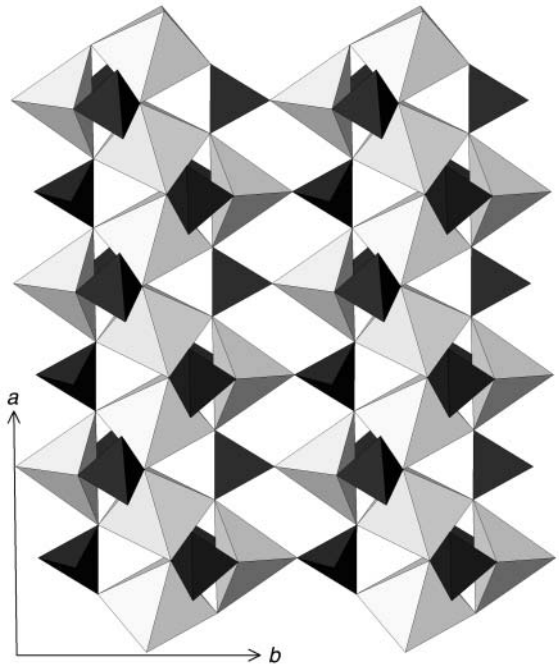

Fig. 2 View of $[Mn_2(HPO_4)_3]\cdot(NH_3(CH_2)_2NH_3)_{3/2}\cdot H_2PO_4$ along the *c* axis showing the manganese-phosphate layer constructed from MnO_6 and MnO_5 polyhedra (light-grey shading) and PO_4 tetrahedra (dark-grey shading) (drawing package: ATOMS[20]).

Table 5 Selected bond distances (Å) and angles (°) for $[Mn_2(HPO_4)_3]\cdot(NH_3(CH_2)_2NH_3)_{3/2}\cdot H_2PO_4$

Mn(1)–O(1)/O(1)^a	2.250(2)	Mn(3)–O(2)	2.124(2)
Mn(1)–O(5)/O(5)^a	2.181(2)	Mn(3)–O(6)	2.120(2)
Mn(1)–O(10)/O(10)^a	2.146(2)	Mn(3)–O(9)^b	2.277(2)
Mn(2)–O(1)/O(1)^b	2.181(2)	Mn(3)–O(10)^a	2.242(2)
Mn(2)–O(5)/O(5)^b	2.237(2)	Mn(3)–O(11)^c	2.033(2)
Mn(2)–O(9)/O(9)^b	2.179(2)		
P(1)–O(1)	1.536(2)	P(2)–O(5)	1.544(2)
P(1)–O(2)	1.524(2)	P(2)–O(6)	1.531(2)
P(1)–O(3)	1.535(2)	P(2)–O(7)	1.516(2)
P(1)–O(4)	1.561(2)	P(2)–O(8)	1.574(2)
P(3)–O(9)	1.531(2)	P(4)–O(13)	1.523(15)
P(3)–O(10)	1.533(2)	P(4)–O(14)	1.485(11)
P(3)–O(11)	1.503(2)	P(4)–O(15)	1.566(15)
P(3)–O(12)	1.588(2)	P(4)–O(16)	1.593(11)
P(5)–O(17)	1.519(7)	O(4) to H(1)	0.96(4)
P(5)–O(18)	1.603(8)	O(8) to H(2)	0.95(4)
P(5)–O(19)	1.551(6)	O(12) to H(3)	0.93(4)
P(5)–O(20)	1.499(7)		
N(1)–C(1)	1.448(6)	C(1)–C(1)^d	1.525(7)
N(2)–C(2)	1.484(5)	C(2)–C(3)	1.465(15)
N(3)–C(3)	1.479(16)	C(2)–C(4)	1.564(8)
N(4)–C(4)	1.492(7)		
O(1)–Mn(1)–O(1)^a	180	O(1)–Mn(2)–O(1)^b	180
O(1)–Mn(1)–O(5)	77.38(8) × 2	O(1)–Mn(2)–O(5)	77.66(8)
O(1)–Mn(1)–O(5)^a	102.62(8)	O(1)–Mn(2)–O(5)^b	102.34(8)
O(1)^a–Mn(1)–O(5)	102.62(8)	O(1)–Mn(2)–O(5)	102.34(8)
O(5)–Mn(1)–O(5)^a	180	O(5)–Mn(2)–O(5)^b	180
O(1)–Mn(1)–O(10)	93.39(8) × 2	O(1)–Mn(2)–O(9)	93.70(8) × 2
O(1)–Mn(1)–O(10)^a	86.61(8)	O(1)–Mn(2)–O(9)^b	86.30(8)
O(5)–Mn(1)–O(10)	93.04(8) × 2	O(5)–Mn(2)–O(9)	94.91(8) × 2
O(5)–Mn(1)–O(10)^a	86.96(8)	O(5)–Mn(2)–O(9)^b	85.09(8)
O(1)^a–Mn(1)–O(10)	86.61(8)	O(1)^b–Mn(2)–O(9)	86.30(8)
O(5)^a–Mn(1)–O(10)	86.96(8)	O(5)^b–Mn(2)–O(9)	85.09(8)
O(10)–Mn(1)–O(10)^a	180	O(9)–Mn(2)–O(9)^b	180
O(2)–Mn(3)–O(6)	170.85(8)	Mn(1)–O(1)–Mn(2)	97.23(8)
O(2)–Mn(3)–O(9)^b	88.73(8)	Mn(1)–O(1)–P(1)	130.0(1)
O(6)–Mn(3)–O(9)^b	87.15(8)	Mn(2)–O(1)–P(1)	125.5(1)
O(2)–Mn(3)–O(10)^a	86.24(8)	Mn(3)–O(2)–P(1)	112.6(1)
O(6)–Mn(3)–O(10)^a	90.42(8)	Mn(1)–O(5)–Mn(2)	97.65(8)
O(9)^b–Mn(3)–O(10)^a	131.81(7)	Mn(1)–O(5)–P(2)	127.5(1)
O(2)–Mn(3)–O(11)^c	87.69(8)	Mn(2)–O(5)–P(2)	129.4(1)
O(6)–Mn(3)–O(11)^c	101.37(8)	Mn(3)–O(6)–P(2)	111.8(1)
O(9)^b–Mn(3)–O(11)^c	109.06(9)	Mn(2)–O(9)–Mn(3)^b	103.34(9)
O(10)^a–Mn(3)–O(11)^c	118.55(8)	Mn(2)–O(9)–P(3)	127.6(1)
		Mn(3)^b–O(9)–P(3)	124.4(1)
P(1)–O(4)–H(1)	116.6(34)	Mn(1)–O(10)–Mn(3)^a	103.52(9)
P(3)–O(12)–H(3)	108.0(35)	Mn(1)–O(10)–P(3)	131.5(1)
P(2)–O(8)–H(2)	110.3(35)	Mn(3)^a–O(10)–P(3)	122.9(1)
		Mn(3)^e–O(11)–P(3)	152.2(1)

O–P–O angles lie in the range 106.8(1) to 112.6(1)° in P(1)O_4, P(2)O_4 and P(3)O_4 tetrahedra and 99.2(4) to 116.6(7)° in P(4)O_4 and P(5)O_4 tetrahedra. Note: Symmetry transformations used to generate equivalent atoms: $^a -x, -y, -z$; $^b 1-x, -y, -z$; $^c x, 1+y, z$; $^d -x, -y, 1-z$; $^e x, 1-y, z$.

are three connected and bond to one phosphorus and two manganese atoms.

Ethylenediammonium cations and $H_2PO_4^-$ units occupy the space between the manganese-phosphate layers (Fig. 3). The $H_2PO_4^-$ units and one of the two crystallographically distinct ethylenediamine cations are disordered over two sites. A complicated network of hydrogen bonds involving $H_2PO_4^-/H_2PO_4^-$ (O(13)···O(15), 2.557(10); O(14)···O(14′), 2.652(14); O(17)···O(19), 2.541(7) Å), $H_2PO_4^-$/diamine (O···N distances in the range 2.473(8)–2.910(8) Å), $H_2PO_4^-$/MnPO-layer (O(18)···O(3), 2.592(4) and O(16)···O(3), 2.659(4) Å) and diamine/MnPO-layer (N···O distances in the range 2.769(4)–2.978(11) Å) interactions serve to hold the structure together (Fig. 3). Isolated $H_2PO_4^-$ units, although rare in open-framework phosphates, have been observed previously in the layered AlPO, $[Al_2(HPO_4)_3F_2]\cdot(N_4C_6H_{21})\cdot H_2PO_4$.[21]

Magnetic characterisation of $[Mn_2(HPO_4)_3]\cdot(NH_3(CH_2)_2NH_3)_{3/2}\cdot H_2PO_4$

The fc and zfc magnetic susceptibility data obtained for $[Mn_2(HPO_4)_3]\cdot(NH_3(CH_2)_2NH_3)_{3/2}\cdot H_2PO_4$ overlie each other over the entire range of temperature studied (Fig. 4(a)). High-temperature data ($T \geqslant 25$ K) follow Curie–Weiss behaviour. The best fit to the inverse susceptibility data (Fig. 4(b)) yields a Curie constant of $C = 8.33(1)$ cm^3 K mol^{-1} and a Weiss constant of $\theta = -30(1)$ K. The former corresponds to an effective magnetic moment per Mn ion of $\mu_{eff} = 5.77(1)\ \mu_B$, which is slightly reduced from the spin-only moment of 5.92 μ_B expected for high-spin Mn^{2+}. The negative Weiss constant indicates that the dominant magnetic exchange interactions are antiferromagnetic in origin. A maximum in the magnetic susceptibility, which is observed at 2.5(1) K, suggests that these interactions result in the establishment of an antiferromagnetically ordered state at low

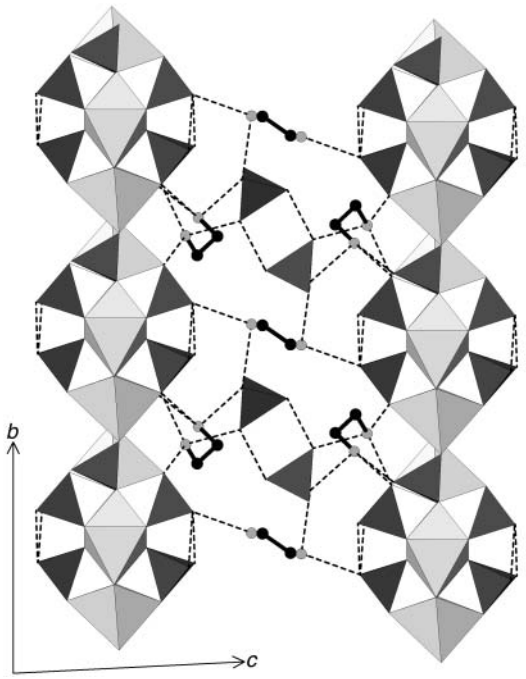

Fig. 3 View of title compound along the *a* axis showing the location of isolated $H_2PO_4^-$ tetrahedra and ethylenediammonium cations in the space between two manganese-phosphate layers. The $H_2PO_4^-$ units and one of the two crystallographically distinct ethylenediammonium cations are disordered over two sites, but for clarity only one of these sites is shown in each case. P–OH···O and NH···O hydrogen-bonding interactions are represented by dotted lines. Key: polyhedra as for Fig. 2, N: grey spheres, C: black spheres, H atoms have been omitted: (drawing package: ATOMS[20]).

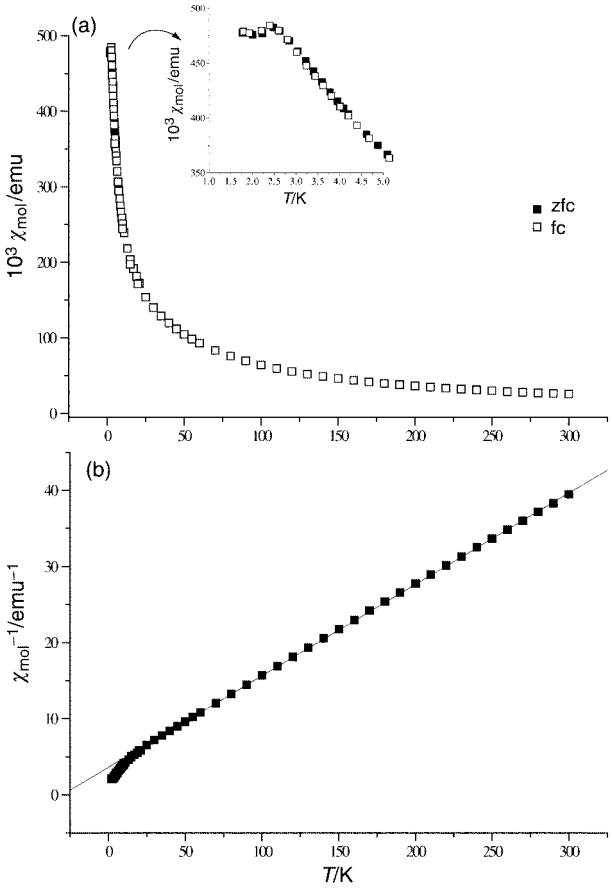

Fig. 4 (a) Temperature dependence of the field-cooled (fc) and zero field-cooled (zfc) molar magnetic susceptibility of $[Mn_2(HPO_4)_3]\cdot(NH_3(CH_2)_2NH_3)_{3/2}\cdot H_2PO_4$ with a measuring field of 1000 G. (b) Reciprocal molar magnetic susceptibility of $[Mn_2(HPO_4)_3]\cdot(NH_3(CH_2)_2NH_3)_{3/2}\cdot H_2PO_4$. Points represent field-cooled data and the straight line is the best fit to the Curie–Weiss expression over the temperature range $25 \leqslant T/K \leqslant 300$.

temperature although the large value of $|\theta|/T_N$ is indicative of a high degree of frustration.[22,23] Antiferromagnetic ordering results in a continuous decrease in the quantity χT with decreasing temperature (Fig. 5). Examination of the structure suggests that magnetic interactions between adjacent manganese-phosphate layers, which are 14.43 Å apart, are likely to be weak, and that the magnetic exchange is dominated by intralayer interactions, primarily those within individual manganese–oxygen zigzag chains (Fig. 2), owing to the relatively large inter-chain separation of 4.47 Å. Within these chains, the manganese sub-lattice consists of a series of corner-linked triangles (Fig. 6), in which the Mn···Mn distances are 3.326(1), 3.447(1) and 3.496(1) Å. These separations are too large for significant direct magnetic exchange to occur, suggesting that coupling occurs *via* the intervening oxygen anions. The two MnO_6 octahedra within the chains share a common edge and hence there are two possible Mn(1)–O–Mn(2) superexchange pathways with cation–anion–cation angles of *ca.* 97°. The 5-coordinate manganese ion, Mn(3), is linked *via* two common anions to each of the octahedral manganese ions with bond angles of *ca.* 103°. Correlation superexchange between two high-spin d^5 ions, *via* anion p-orbitals, is predicted to be antiferromagnetic for all angles in the range 90–180°, in accordance with the negative Weiss constant.[24] For a triangular array of antiferromagnetically coupled moments, it is not possible, owing to topological constraints, to satisfy the requirement that all nearest neighbour moments are aligned antiparallel.[23,25] This frustration induces a rotation of neighbouring moments, and it has been shown that the lowest energy configuration for a trinuclear triangular complex is a co-planar array in which the moments are aligned at 120° to those of their neighbours.[26] Deviations from this ideal configuration have been observed in two-dimensional triangular networks[27] and Lacorre has demonstrated that the spin configuration is a sensitive function of the individual exchange constants.[28] In the present case, neutron diffraction data would be required to establish the nature of the low-temperature magnetically ordered structure.

Rushbrooke and Wood[29] have derived expressions for the temperature variation of the magnetic susceptibility for a

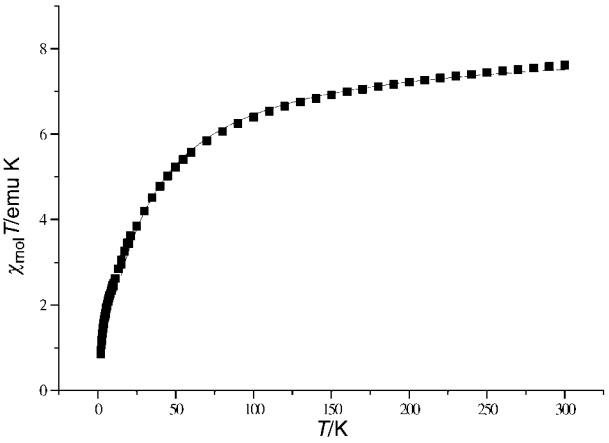

Fig. 5 Temperature variation of the quantity $\chi_{mol}T$, illustrating the decrease in effective magnetic moment with decreasing temperature. The solid line represents the fit to the field-cooled data over the temperature range $15 \leqslant T/K \leqslant 300$ using the equation given in the text.

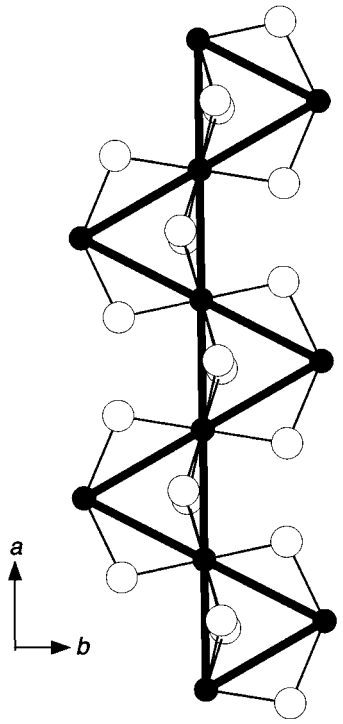

Fig. 6 A chain of corner-linked Mn_3 triangles in $[Mn_2(HPO_4)_3]\cdot(NH_3(CH_2)_2NH_3)_{3/2}\cdot H_2PO_4$, illustrating the possible Mn–O–Mn superexchange pathways (drawing package: ATOMS[20]).

number of topologically different lattices, in which the couplings between nearest neighbour moments are isotropic and the exchange interactions are described by the Heisenberg Hamiltonian. Given the similarity of the three superexchange pathways in $[Mn_2(HPO_4)_3]\cdot(NH_3(CH_2)_2NH_3)_{3/2}\cdot H_2PO_4$, the individual exchange constants may be approximated by a single parameter, J, and the temperature dependence of the susceptibility described by the following expression appropriate to a triangular lattice:

$$\chi_m = (35N\beta^2g^2/12kT)(1+35x+221.667x^2-1909.83x^3 +6156.92x^4+84395.9x^5-1522000x^6)^{-1}$$

where $x=|J|/kT$, k is the Boltzmann constant, N is the number of magnetic ions per mole and β is the Bohr magneton. This expression was fitted to the data over the temperature range $15\leqslant T/K\leqslant 300$ and the best fit to χT (Fig. 5) was obtained with the parameters $g=1.930(3)$ and $J/k=-0.72(1)$ K. These values are in good agreement with the corresponding values of 1.977 and −0.75 K determined for the structurally related phase $[Mn_2(HPO_4)_3](NH_3CH_2CH_2NH_3)(H_2O)$.[9] The exchange constant is significantly lower than $J/k=-2.98$ K determined for the coupling between divalent manganese ions in the phosphate MnGaPO-2.[5] In the latter compound, pairs of manganese ions are linked by four phosphate groups to form dimers in which the Mn···Mn separation is *ca.* 3.5 Å. The stronger exchange interaction raises the antiferromagnetic ordering temperature in MnGaPO-2 to 10(1) K.

Washed product, $[Mn_2(HPO_4)_3](NH_3CH_2CH_2NH_3)(H_2O)_x$

The choice of solvent for washing the bulk products of reactions (i) and (ii) is clearly important. Use of acetic acid followed by methanol led to preservation of $[Mn_2(HPO_4)_3]\cdot(NH_3(CH_2)_2NH_3)_{3/2}\cdot H_2PO_4$ as either single crystals (reaction (i)) or in polycrystalline form (reaction (ii)). Treatment of both products with water however led to the formation of polycrystalline samples of a new phase of formula $[Mn_2(HPO_4)_3]\cdot(NH_3(CH_2)_2NH_3)\cdot(H_2O)_x$ ($x\sim0.2$) with an A-centred monoclinic unit cell. The lattice parameters of the washed product are very similar to those determined from single-crystal X-ray data for $[Mn_2(HPO_4)_3](NH_3CH_2CH_2NH_3)(H_2O)$ ($a=6.639(2)$, $b=9.345(1)$, $c=21.961(7)$ Å, $\beta=91.06(2)^\circ$)[9] although the latter material crystallises in primitive spacegroup $P2_1/n$ suggesting some structural differences between the two phases.

The a and b lattice parameters for $[Mn_2(HPO_4)_3]\cdot(NH_3(CH_2)_2NH_3)\cdot(H_2O)_x$ are similar to those found for $[Mn_2(HPO_4)_3]\cdot(NH_3(CH_2)_2NH_3)_{3/2}\cdot H_2PO_4$ suggesting that the manganese-phosphate layers are retained on washing. There is a decrease in interlayer separation from ~14.43 to 11.02 Å consistent with the proposal, supported by chemical analysis, that two-thirds of the ethylenediammonium cations have been retained but the interlayer $H_2PO_4^-$ groups and associated diamine cations have been removed and replaced, in part, by water molecules. Further work is in progress to determine whether other amines can be inserted between the manganese-phosphate layers.

Acknowledgements

A. M. C. thanks the EPSRC for Research Grant GR/N37490 and the University of Reading for an RETF Senior Research Fellowship and the Royal Society of Chemistry for a Research Grant. A. R. C. thanks the EPSRC for a Research Studentship. Miss K. J. Peacock is also thanked for preliminary synthetic studies.

References

1 A. K. Cheetham, G. Férey and T. Loiseau, *Angew. Chem., Int. Ed.*, 1999, **38**, 3268.
2 M. Hartmann and L. Kevan, *Chem. Rev.*, 1999, **99**, 635.
3 A. M. Chippindale and A. R. Cowley, *Microporous Mesoporous Mater.*, 1998, **21**, 271.
4 A. D. Bond, A. M. Chippindale and A. R. Cowley, *Zeolites*, 1997, **19**, 326.
5 A. M. Chippindale, A. D. Bond, A. R. Cowley and A. V. Powell, *Chem. Mater.*, 1997, **9**, 2830.
6 A. M. Chippindale, A. R. Cowley and A. D. Bond, *Acta Crystallogr.*, 1998, **C54**, CIF access paper IUC9800061.
7 K. F. Hsu and S. L. Wang, *Chem. Commun.*, 2000, 135.
8 K. F. Hsu and S. L. Wang, *Inorg. Chem.*, 2000, **39**, 1773.
9 J. Escobal, J. L. Pizarro, J. L. Mesa, L. Lezama, R. Olazcuaga, M. I. Arriortua and T. Rojo, *Chem. Mater.*, 2000, **12**, 376.
10 K. O. Kongshaug, H. Fjellvag and K. P. Lillerud, *J. Solid State Chem.*, 2001, **156**, 32.
11 A. I. Vogel, in *Textbook of Quantitative Chemical Analysis*, 5th edn., Longman Group, UK, 1989.
12 M. T. Averbuch-Pouchot and A. Durif, *Acta Crystallogr.*, 1987, **C43**, 1894.
13 K. Nakamoto, in *Infrared and Raman Spectra of Inorganic and Coordination Compounds*, 5th edn, John Wiley and Sons, New York, 1997.
14 Z. Otwinowski and W. Minor, in *Processing of X-ray Diffraction Data Collected in Oscillation Mode, Methods Enzymol.*, ed. C. W. Carter and R. M. Sweet, Academic Press, 1997, vol. 276.
15 *International Tables for Crystallography*, ed. T. Hahn, Kluwer Academic Publishers, Dordrecht, The Netherlands, 1995.
16 A. Altomare, M. C. Burla, M. Camalli, G. Cascarano, G. Giacovazzo, A. Guargliardi and G. Polidori, *J. Appl Crystallogr.*, 1994, **27**, 435.
17 D. J. Watkin, C. K. Prout, J. R. Carruthers and P. W. Betteridge, CRYSTALS issue 10, Chemical Crystallography Laboratory, Oxford, 1996.
18 L. J. Pearce, C. K. Prout and D. J. Watkin, *CAMERON User Guide*, Chemical Crystallography Laboratory, Oxford, 1993.
19 N. E. Brese and M. O'Keefe, *Acta Crystallogr.*, 1991, **B47**, 192.
20 E. Dowty, ATOMS for Windows, V. 4.0, Shape Software, 521 Hidden Valley Road, Kingsport, TN 37663, 1997.
21 N. Simon, T. Loiseau and G. Férey, *J. Mater. Chem.*, 1999, **9**, 585.
22 A. P. Ramirez, *Annu. Rev. Mater. Sci.*, 1994, **24**, 453.

23 J. M. Greedan, *J. Mater. Chem.*, 2001, **11**, 37.
24 J. B. Goodenough in *Magnetism and the Chemical Bond*, Wiley, New York, 1963.
25 *Magnetic Systems with Competing Interactions (Frustrated Spin Systems)*, ed. H. Diep, World Scientific, Singapore, 1994.
26 N. Uryu and S. A. Friedberg, *Phys. Rev.*, 1965, **140**, A1803.
27 P. Lacorre, M. Leblanc and G. Férey, *J. Mag. Magn. Mater.*, 1987, **66**, 219.
28 P. Lacorre, *J. Phys. C: Solid State Phys.*, 1987, **20**, L775.
29 G. S. Rushbrooke and P. J. Wood, *Mol. Phys.*, 1958, **1**, 257.